Rev.Adv.Mater.Sci. 18(2008) 23-26

STRAIN RATE EFFECT ON DEFORMATION OF Zr-BASED METALLIC GLASS: IN-SITU TENSILE DEFORMATION IN SEM ANALYSIS

K. Hajlaoui[1,2], M. Stoica[1], A. LeMoulec[1], F. Charlot[1] and A.R. Yavari[1]

[1]Institut National Polytechnique de Grenoble, St. Martin d'Hères 38402, France.
[2]Ecole Nationale D'Ingénieurs de Sousse, Cité Ibn Khouldoun, 4003 Sousse, Tunisie

Received : March 29, 2008

Abstract. In-situ tensile tests performed in a scanning electron microscope (SEM) were used to study mechanical behavior of a Zr-Bulk metallic glass and highlight the effect of strain rate. Shear band generation and propagation was observed at several stages of deformation. Fracture surface was analyzed immediately after rupture under SEM secondary vacuum, avoiding contamination of sample surface. We found that contrary to experimental results performed in constrained geometries such as in compression or indentation, increasing strain rate in tension leads to formation of multiple parallel shear bands and enhanced macroscopic plasticity up to 1.5% with slight decrease of elastic strength and Young modulus. Fracture surface analysis revealed that flow is an accommodation mechanism for deformation in metallic glasses.

1. INTRODUCTION

The need for fundamental understanding the flow in metallic glasses has motivated a variety of experimental investigations involving temperature and strain-rate sensitivities [1-3] and assessing the dependence of flow on microstructure and heat treatment [4-6]. In parallel, theoretical models helped to explain various features of homogeneous and heterogeneous flow. Flow in metallic glasses is inhomogeneous at low temperature and high strain rates [7]. Plastic deformation is highly localized into shear bands, which initiate and propagate rapidly across the sample and cause macroscopic fracture. However, it has been recently shown that in some cases [1], metallic glass ribbons can undergo enhanced microscopic ductility associated with multiple shear bands generation. This result seems to be interesting for approaching the strain localization in metallic glasses and plastic deformation, related with state. In this paper, we study the influence of strain rate on both, tensile strength and ductility of a $Zr_{55}Cu_{20}Ti_5Al_{10}Ni_{10}$ bulk metallic glass (BMG). Formation and growth of shear bands as well as fracture morphology for the BMG was analyzed through in situ tensile tests.

2. EXPERIMENTAL DETAILS.

$Zr_{55}Cu_{20}Ti_5Al_{10}Ni_{10}$ BMG (nominal composition in atomic percent) was chosen in this work. The master alloy was produced by arc melting together the pure elements under a purified argon atmosphere and then the ingot was remelted several times to ensure a homogeneous composition. Plates of 11 x 30 x 1 mm^3 of the metallic glass were made by suction casting the molten alloy into a copper mold. The amorphous structure of these plates was checked by standard x-ray diffraction (XRD) using a Siemens Kritalloflex D500 diffractometer and Cu-K_α radiation. Tensile specimens 12 mm in gauge length, 1.5 mm in gauge width, 1 mm thickness and 2 mm in shoulder radius were electrode discharge machined from the amorphous plate (Fig. 1).

Corresponding author: K. Hajlaoui, e-mail: k.hajlaoui@yahoo.fr, euronano@ltpcm.inpg.fr

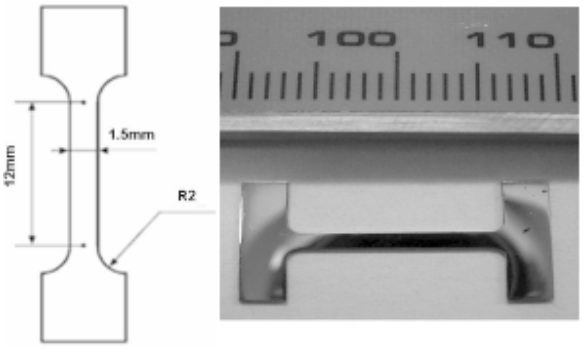

Fig. 1. Shape of tensile specimens used in the present study.

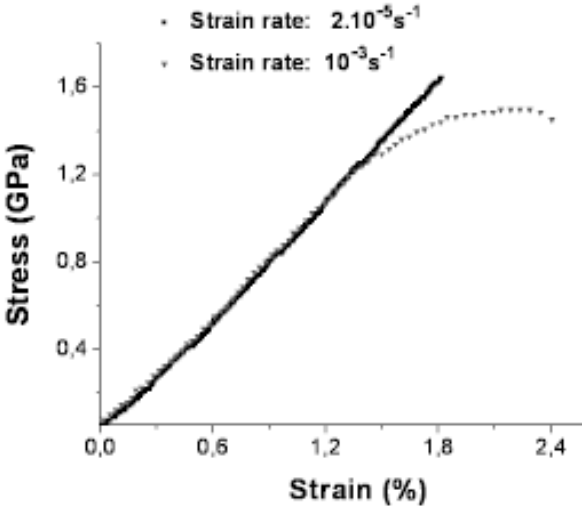

Fig. 2. Stress– strain curves at two different strain rates.

Specimen surfaces were mechanically polished with silica papers to reduce the thickness to about 0,5 mm. The ground surfaces were also mechanically polished with alumina slurry to eliminate scratches produced during machining. In situ tensile tests were carried out in a JEOL 6400 SEM equipped with a tensile stage device at room temperature. The strain rate was fixed, and load-displacement data were recorded in two ways with analogue and digital signals. After failure, the specimen and the fracture surfaces were directly observed by SEM in vacuum.

3. RESULTS AND DISCUSSIONS

Stress–strain curves for the alloy at room temperature and at two different strain rates are shown in Fig. 2. The curve for strain rates 2 10^{-5} s^{-1} is characterized by the absence of plastic yielding that is common metallic glass behavior at room temperature. The yield stress and elastic strain are around 1700 MPa and 1,9% respectively with no plastic deformation. However, for high strain rate (10^{-3} s^{-1}), plastic elongation of about 1-1,5 % has been revealed. This is associated with clear decrease in fracture stress and elastic strain range.

While the decrease of flow stress as a function of strain rate has been reported both in tensile and in compression [8-11], the increase of plasticity, especially at high strain rates, has been observed only in tensile configuration and reported in [1], as was found also in the present work.

3.1. Fracture behavior

The fracture surface and the external surface were observed simultaneously in SEM by tilting the specimen. Fig. 3a is a side view of the sample fractured at the strain rate of 2 10^{-5} s^{-1}. It is observed that samples fracture proceeds along a single plane, indicating that one major shear band dominates the final fracture. The fracture plane is inclined at 54° with respect to the tensile axis. A 54° inclination angle in tension has also been reported by other researchers [12].

Fig. 3b is a lower magnification secondary electron (SE) image of external surface of a specimen strained at 2 10^{-5} s^{-1}. Many vertical stripes consisting of ridges and valleys are observed. The specimens used in this work have shoulders for hooking over the specimen holders, as shown in Fig. 1, so that stress should be strongly concentrated at the boundaries between the shoulders and the gauge section. In fact, shear bands were more frequently generated on the shoulders side rather than on the gauge as seen in Fig. 3b. So, when stress concentration occurs under certain local condition, a shear (mode II) microcrack will initiate in the weakened shear plane. When the shear crack grows along the shear band into 20/25 μm in depth, it will open and become a shallow I-II complex crack under a normal stress component. As soon as the complex crack becomes a mode I crack penetrating the thickness it will propagate rapidly along the width until fracture of the specimen.

SEM observations of the gauge surfaces of the samples deformed at the lower strain rate revealed secondary shear bands and multiple cracks near

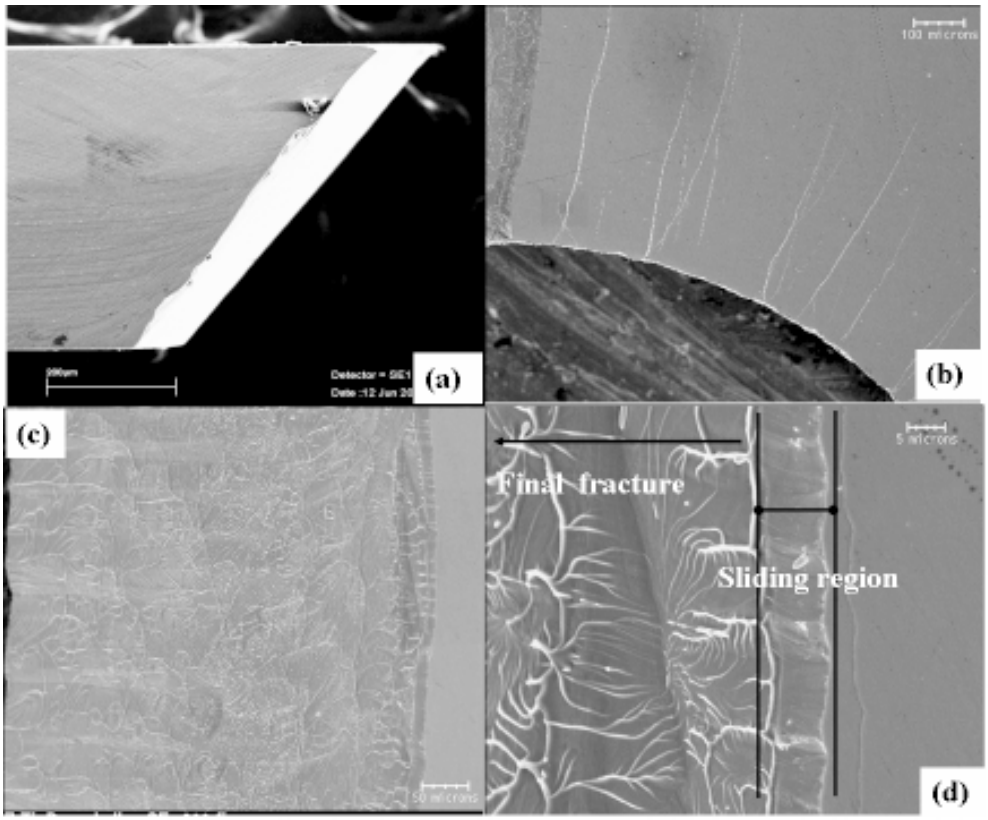

Fig. 3. (a) Side surface of the specimen fractured at the strain rate of 2 10^{-5} s^{-1} (b) Forming and growing of shear band (side-view), (c) and (d) Fracture surfaces (planar-view) in the vicinity of the sample edge for samples deformed in tension.

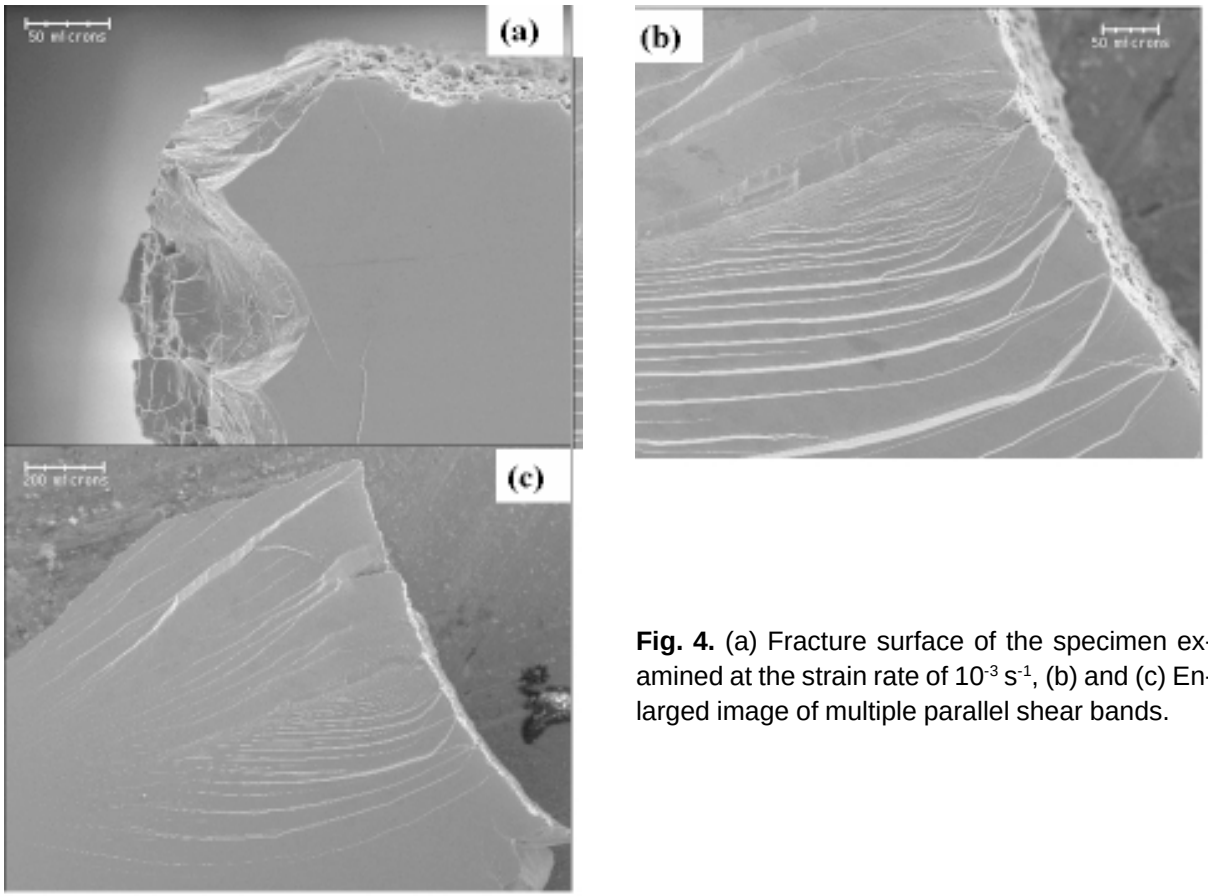

Fig. 4. (a) Fracture surface of the specimen examined at the strain rate of 10^{-3} s^{-1}, (b) and (c) Enlarged image of multiple parallel shear bands.

the fracture surfaces (Fig. 3b), which are believed to be formed during rapid crack propagation along the primary shear band. These tests at lower strain rates did not exhibit ductility in tension. Fracture surfaces in the vicinity of the sample edge are shown in Figs. 3c and 3d. A small sliding region is seen before the onset of the final catastrophic fracture (i.e. the vein pattern).

Fracture surfaces of samples deformed at high strain rates (10^{-3} s^{-1}) have a quite different appearance. The fracture surface and side surface of the specimen are shown in Figs. 4a, 4b, and 4c, respectively. In contrast to a simple shear-off surface appearance in sample fractured at low strain rate, the fracture surface of the sample tested at high strain rate is relatively rough. Close examination of the side surface reveals the presence of parallel shear bands. This suggests the simultaneous operation of multiple shear bands at the dynamic strain rate. In contrast to the observation of shear banding localization to the area of fracture at lower strain rate, additional multiple shear bands parallel to the primary one (along which fracture occurred) were detected away from the fracture surface (Figs. 4b and 4c) at the higher rate. The results suggest that flow is a stress relaxation process. In fact, in tensile configuration, once the shear band begins to propagate, fracture rapidly follows. If the nucleation rate is faster than the applied strain rates, then a weak or no strain rate effect is expected. This is the case of some published data using a very limited strain rate range [12,13]. However, at sufficient high strain rate, the rate of shear band nucleation is not sufficient enough to accommodate the applied strain rate and, thus, additional shear bands must be formed in order to accommodate the large amounts of imposed strain in a much smaller time frame. With shear bands, a step-like relief forms in a large portion the sample (Figs. 4b and 4c). The presence of large numbers of shear bands is then associated with an increase in ductility as shown in Fig. 2.

4. CONCLUSION

Mechanical behavior of a $Zr_{55}Cu_{20}Ti_5Al_{10}Ni_{10}$bulk metallic glass has been investigated through in situ tensile tests in scanning electron microscope for two different strain rates. Following observations were made.

-An increase of 1-1,5% plasticity is observed in the stress-strain curves at high strain rate linked with diminishing of fracture stress and elastic strain. Fracture surface and external surfaces were different for high and low strain rate.

-Secondary shear bands and multiple cracks near the fracture surfaces were observed at high strain rate. The macroscopic plasticity of metallic glasses at room temperature is a summation of local strains contribution of every shear band in the gauge section.

- The lack of ductility in the tensile tests in the literature could be due to sensitivity to a critical strain rate, which may be material-related (structure) and may depend on stress states.

ACKNOWLEDGEMENTS

This work was performed in the framework of the EU Network on bulk metallic glass composites (MRTN-CT-2003-504692 <Ductile BMG Composites>) coordinated by A.R. Yavari.

REFERENCES

[1] A.V. Sergueeva, N.A. Mara, D.J. Branagan and A.K. Mukherjee // *Scr. Mater* **50** (2004) 1303.

[2] C.A. Schuh and T.G. Nieh // *Acta. Mater.* **51** (2003) 87.

[3] J.J. Lewandowski and A.L. Greer // *Nature Mater* **5** (2006) page 15.

[4] A.R. Yavari, A. Le Moulec, A. Inoue and N. Nishiyama // *Acta Mater.* **53** (2005) 1611.

[5] K. Hajlaoui, T. Benameur, G. Vaughan and A.R. Yavari // *Scri Mater.* **51** (2004) 843.

[6] K. Hajlaoui, A.R. Yavari, B. Doisneau and A. LeMoulec // Scri. Mater. **54** (2006) 1829.

[7] F.A. Spaepen // *Acta Metall.* **25** (1977) 407.

[8] T.G. Mukai, Y. Nieh, Y. Kawamur, A. Inoue and K. Higashi // *Intermetallics* **10** (2002) 1071.

[9] Y. Kawamura, T. Shibata, A. Inoue and T., Masumoto // *Scripta Mater* **37** (1997) 431.

[10] G. Subhash, R.J. Dowding and L.J. Kecskes // *Mater Sci Eng A* **334** (2002) 33.

[11] T.C. Hufnagel, T. Jiao, Y. Li, L.Q. Xing and K.T. Ramesh // **17** *J Mater Res* (2002)1441.

[12] Z.F. Zhang, J. Eckert and L. Schultz // *Acta Materialia* **51** (2003) 1167.

[13] T. Mukai, T.G. Nieh, Y. Kawamura, A. Inoue and K. Higashi // *Scri. Mater* **46** (2002) 43.